

On-Site Application of End-Grain Bonded Timber Under Low Curing Temperatures

Dio Lins*, Steffen Franke

Bern University of Applied Sciences, Solothurnstrasse 102, 2504 Biel/Bienne, Switzerland

*Corresponding author: dio.lins@bfh.ch

<https://doi.org/10.5755/j01.sace.34.1.35788>

The end-grain bonding of timber components using the Timber Structures 3.0 technology (TS3) is an advancing construction method in timber engineering. This technology allows the realisation of any plate size by bonding plates on-site where low temperatures influence the performance. Therefore, investigations are underway to evaluate the influence of the low temperatures on the curing process. Additionally, research is in progress to discover techniques to reduce any adverse effects of low curing temperatures on the mechanical properties of the bond. The implementation of particular measures, such as the inclusion of milled heating wires into the joint and the pre-heating of the joint with a hot air blower, has been identified as advancing the potential for grouting even in the face of low external temperatures, as recent research has indicated.

Keywords: cross-laminated timber; CLT; flat slabs; end-grain bonded timber; on-site application; temperature effect.

End-Grain Bonding of Timber Components with the TS3-technology

Throughout history, the use of wood in construction has been limited to uniaxial load-bearing applications. It was only around thirty years ago, with the emergence of Cross-Laminated Timber (CLT), that the possibility of biaxial load-bearing timber components became apparent. However, because of limitations in transportation and manufacture, which restrict CLT elements to dimensions of around 3 m x 12 m, and the inability of on-site joining methods to offer a flexurally rigid connection of individual boards, the complete biaxial load-bearing capacity of CLT remains unrealised.

The incorporation of the Timber Structures 3.0 technology (TS3) and its end-grain bonding has resulted in a crucial development for the construction industry. Its capability to provide a flexurally rigid connection of elements on-site creates a high-performance and competitive timber product that has the potential to surpass reinforced concrete floors. This novel technology presents significant progress and is showcased in Fig. 1 and Fig. 2. This marks a significant step forward in promoting sustainable building practices. Wood, used as a building material, presents a clear alternative to reinforced concrete, which necessitates substantial primary energy during its fabrication - particularly in the process of cement production - and therefore emits high levels of CO₂. Compared to reinforced concrete, wood as a building product generally has a much lower primary energy requirement, and wood also has the added benefit of sequestering around 1 tonne of CO₂ per cubic metre.

JSACE 1/34

On-Site
Application of
End-Grain Bonded
Timber Under
Low Curing
Temperatures

Received
2023/12/03

Accepted after
revision
2024/01/23

Abstract

Introduction



Fig. 1

TS3 Building: Columns, Slabs, Ready (source: <https://www.ts3.biz/en/technologien/>)

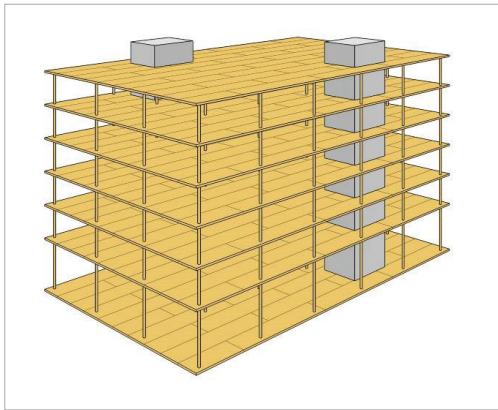


Fig. 2

CLT Joint with TS3 Technology (source: <https://www.ts3.biz/en/technologien/>)

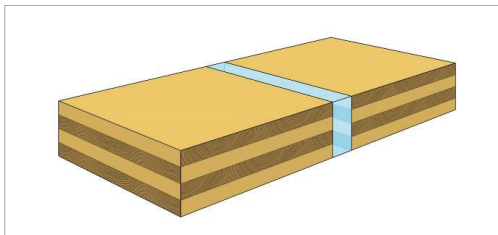


Fig. 3

Apartment Building with wooden basement, Thun (source: <https://www.ts3.biz/en/referenzprojekte/>)



Fig. 4

Apartment Houses, Grossaffoltern (source: <https://www.ts3.biz/en/referenzprojekte/>)



The end-grain bonding process is carried out as follows: (1) The precision cutting of cross-laminated timber elements to the required dimensions is done at the manufacturing facility followed by the pre-treatment. This involves carefully applying a two-component polyurethane adhesive to the designated surface areas. (2) The prepared cross-laminated timber panels are delivered on-site, positioned and secured with a 4 mm gap in between. (3) Using a specialised application device, the casting resin is systematically injected into the joint through the filler hole, efficiently preventing the development of air pockets in the joint.

Reference Projects

The TS3 Technology has been used to construct multiple buildings, mainly in Switzerland, with additional examples in Canada and Austria, as demonstrated in Fig. 3 to Fig. 6. Fig. 3 showcases the TS3 technology in action, utilised even in the wooden basement, connecting the wooden floor slabs to the basement walls of an apartment block. Two of four identical blocks of flats are shown in Fig. 4, made using 2300 square metres of CLT for the floor slabs, all connected with TS3 technology. The TS3 technology is not restricted to regular flat-slab-to-column formations but can also be adapted to more individualistic free-form designs, as displayed in the "Semiramis" project in Fig. 6 presents a test rig at Bern University of Applied Sciences, which also implemented TS3 technology. This structure was able to withstand a load of about 3.3 kN/m². Additionally, the balcony, which was cantilevered, 1 ton loaded, and exposed to weather (SC3 conditions), managed to endure the continuous load without any complications for the bond line.

Challenges of On-site Application

The main construction phase usually took place during warmer seasons so far to prevent negative impacts of cold weather on the joint performance. However, it is imperative to examine on-site application even in lower ambient temperatures to facilitate international dissemination of this technology and offer an eco-friendly substitute for traditional reinforced concrete slabs. The main challenge in construction sites currently remains in achieving the minimum processing tem-

perature of 17 °C, as required by the casting resin manufacturer (Deutsches Institut für Bautechnik, 2020). Unfortunately, this threshold is rarely reached in numerous regions across the European market. This issue is especially prevalent in Scandinavia, where timber constructions are commonly used, as well as in the Baltic States and Central Europe during prolonged periods of cold weather, as shown in Fig. 7.

Lins and Franke (2023) conducted preliminary investigations into the curing characteristics of end-grain bonding in timber components. They uncovered that tensile strength in the bond correlates with curing time and temperature. Lower curing temperatures necessitate extended curing periods to reach the final bond strength (refer to Fig. 8). Moreover, it is evident that this ultimate strength remains lower at lower curing temperatures, even after a prolonged curing period, in comparison to 20 °C, for instance. Subsequently, a potential post-curing effect was explored. The test specimens undergo an additional 14-day post-curing process at a temperature of 20 °C after the 20-day curing period at the corresponding lower temperature. However, there is no observable beneficial impact on the tensile strength after post-curing. The reduction in strength as a result of curing at 0 °C compared to 20 °C is approximately 35% (as illustrated in Fig. 9). These findings clearly underscore the negative impact of low-temperature curing on the mechanical properties of the bond. Consequently, strategies must be developed to ensure full bonding performance even at low temperatures. Only this allows that the geographic applicability can be further expanded without constraints related to the warmer seasons.



Fig. 5

Semiramis, Zug (source: <https://www.ts3.biz/en/referenzprojekte/>)



Fig. 6

Outdoor Test Stand at the Bern University of Applied Sciences, Biel (source: <https://www.ts3.biz/en/referenzprojekte/>)

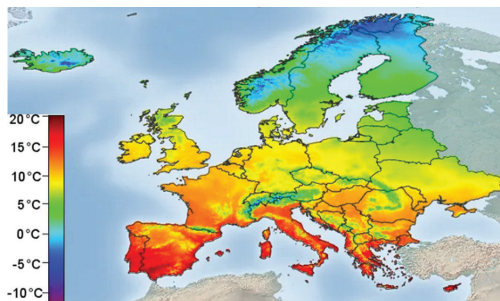


Fig. 7

Average Air Temperature in Europe (source: <https://www.wetter-atlas.de/klima/europa.php>)

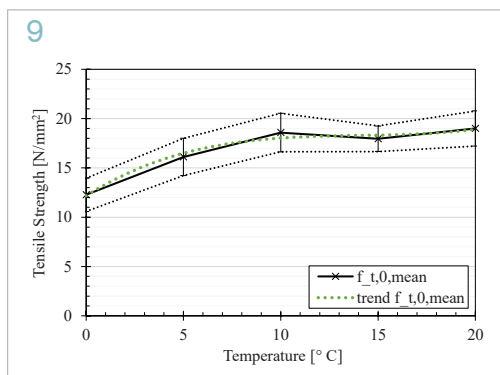
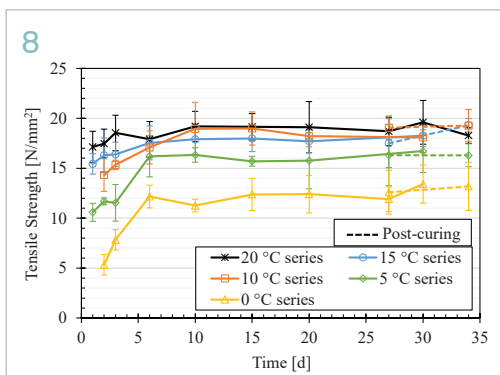


Fig. 8

Tensile Strength vs. Curing Time

Fig. 9

Tensile Strength vs. Curing Temperature

Material and Methods

Solution Approaches

As noted in the challenges section, it has been established that lower temperatures may negatively impact the mechanical properties of end-grain bonding in timber components. Currently, there are no suitable compensation measures available. Therefore, various strategies have been investigated. Two potential methods are under consideration to address the impact of low curing temperatures on the mechanical properties of the end-grain bonded timber. The more elaborate approach incorporates a heating wire into the joint, allowing for precise temperature control, which guarantees effective bonding conditions at low ambient temperatures. An alternative approach involves utilising a hot air blower to direct warm air into the joint through the filling hole prior to the casting process. The aim of this method is to sufficiently preheat the joint, consequently elevating the surface temperature of the wood or pre-treatment and improving the bond between the pre-treatment and casting resin.

Materials

The laboratory experiments employed symmetrical cross-laminated timber elements with a 7-layer layout. The longitudinal layers had a lamella thickness of 40 mm, while the transverse layers measured 30 mm in thickness, leading to a total height of 240 mm. All the conducted tests used spruce wood (*Picea abies*) with a wood moisture content of approximately 12%. A uniform joint thickness of 4 mm was maintained throughout all the experiments. In the heating-wire tests, the joint was filled with TS3 PTS CR192 casting resin. This resin is a two-component polyurethane casting material specifically designed for bonding timber components at the end grain. It shows similar properties to the adhesive used for bonded-in threaded rods in timber components.

Methodology of using milled heating wires

Laboratory Experiments

The initial tests included the installation of milled heating wires. To achieve the curing temperature specified by the manufacturer of 17°C within the joint, or at least at the load-bearing lamellae, the first step involved milling grooves into the 500 mm long cross-laminated timber element, followed by the installation of two heating wires. The grooves were positioned in the non-load-bearing

cross layers, specifically within the third and fifth layer, as shown in Fig. 10. These grooves were 4 mm high and 5 mm deep. Insulated copper strands with a diameter of 3.4 mm were chosen for the heating wires. Furthermore, prior to casting, seven temperature measurement points were installed at different heights across the cross section (see Fig. 11) and connected to a data logger (see Fig. 12). A constant surrounding temperature of 0 °C was maintained by placing the test specimen in a climate chamber (see Fig. 12), while the heating wires were controlled by a power unit to achieve an electrical power of 15 W/m. This enabled the creation and recording of practical temperature curves.

Furthermore, a transient thermal numerical simulation was conducted in ANSYS® to map the test setup. The geometry of the laboratory experiment was used, assuming all con-

Fig. 10

CLT Element with Heating Wires in Grooves in the Cross Layers



Fig. 11

Test Setup: Temperature Sensors and Heating Wires before Casting



tact surfaces were rigidly bonded. The material parameters required for spruce timber, such as thermal conductivity and specific heat capacity, depend on the wood's moisture content (u) and the respective fibre direction. Parameters are taken from literature (e.g., Niemz, 2005) with minor deviations. On the other hand, the values regarding the casting resin were solely obtainable for the cured state and were provided directly by the manufacturer. Although these values differ from those in the fluid or curing state that was modelled, they were used as an initial estimate. As the two-component casting resin undergoes an exothermic reaction, a heat is produced, which also had to be modelled. An assumption derived from the manufacturer's specifications was also considered for this purpose. The heat transfer coefficient (α), which characterises convective heat transfer (Kuchling, 2010), was estimated based on the orientation of the respective surfaces in enclosed spaces (Kuchling, 2010). With the input values provided and an initial and ambient temperature of 0 °C, the temperature distribution was calculated across the cross section over a period of 29 hours.

A sensitivity analysis was conducted to determine the impact and precise values of material parameters of casting resin in liquid or curing states (thermal conductivity, specific heat capacity, and exothermic reaction heat), which are yet to be accurately established. The sensitivity analysis included the heat transfer coefficient (α) due to the significantly higher flow velocity observed in the climate chamber compared to expectations, as well as its minimal dependence on surface orientation. Subsequently, the parameters in the simulation were optimised to achieve agreement between the simulation and experiment.

On-site Validation

To reassess the previously determined parameters and investigate potential variations arising from dissimilarities between laboratory and construction site circumstances, a heating wire was also employed in an actual project. This was followed by conducting temperature measurements. The study employed symmetrical five-layer cross-laminated timber units, with a height of 200 mm and a heating wire inserted in a groove at the lower edge of the middle lamella, similar to laboratory experiments (see Fig. 13). The external temperature was around 5 °C, and the electric power of the heating wire was set to 9 W/m. The timber and casting resin were at 5 and 20 °C, respectively, before casting. Commencing with the casting process, the heating wire was actively engaged for 29 hours during



Fig. 12

Test Setup: Data Logger and Power Unit (above) and cast Test Specimen in the Climate Chamber (below)



Fig. 13

Section of CLT Elements with Heating Wire in the Groove

Fig. 14

Temperature
Sensors On-site

in was introduced at 20 °C. The heating phase was subsequently modelled, and the outcomes were comparatively analysed after 29 hours.

Methodology of Using a Hot Air Blower

The previous method, which included the temporary increase of the surface temperature via a hot air blower prior to the casting process, was subjected to laboratory analysis. A 7-layer CLT test specimen measuring 750 mm in length, as previously detailed, was employed to carry out this investigation. The specimen underwent the standard pre-treatment before drilling a filling hole at the centre of the section length. The hole extended upwards from the upper edge of the lower lamella at an angle of approximately 45° in line with the construction site design. The cross section was equipped with five temperature measuring points (no. 1 - 3 at the end of the section and no. 4 - 5

Fig. 15

Test Setup with
Temperature Sensors

Fig. 16

Hot Air Blower



the curing process. The temperature data acquisition was similar to the laboratory experiment, with 5 measuring points distributed across the cross section (refer to Fig. 14).

Additionally, a corresponding numerical simulation was conducted utilising the predefined parameters, geometry, and boundary conditions of the project. The simulation considered the varying initial temperatures of the materials: the wood was assigned a temperature of 5 °C initially while the casting res-

in was introduced at 20 °C. The heating phase was subsequently modelled, and the outcomes were comparatively analysed after 29 hours.

in was introduced at 20 °C. The heating phase was subsequently modelled, and the outcomes were comparatively analysed after 29 hours.

in was introduced at 20 °C. The heating phase was subsequently modelled, and the outcomes were comparatively analysed after 29 hours.

in was introduced at 20 °C. The heating phase was subsequently modelled, and the outcomes were comparatively analysed after 29 hours.

in was introduced at 20 °C. The heating phase was subsequently modelled, and the outcomes were comparatively analysed after 29 hours.

in was introduced at 20 °C. The heating phase was subsequently modelled, and the outcomes were comparatively analysed after 29 hours.

in was introduced at 20 °C. The heating phase was subsequently modelled, and the outcomes were comparatively analysed after 29 hours.

in was introduced at 20 °C. The heating phase was subsequently modelled, and the outcomes were comparatively analysed after 29 hours.

in was introduced at 20 °C. The heating phase was subsequently modelled, and the outcomes were comparatively analysed after 29 hours.

in was introduced at 20 °C. The heating phase was subsequently modelled, and the outcomes were comparatively analysed after 29 hours.

in was introduced at 20 °C. The heating phase was subsequently modelled, and the outcomes were comparatively analysed after 29 hours.

in was introduced at 20 °C. The heating phase was subsequently modelled, and the outcomes were comparatively analysed after 29 hours.

in was introduced at 20 °C. The heating phase was subsequently modelled, and the outcomes were comparatively analysed after 29 hours.

in was introduced at 20 °C. The heating phase was subsequently modelled, and the outcomes were comparatively analysed after 29 hours.

in was introduced at 20 °C. The heating phase was subsequently modelled, and the outcomes were comparatively analysed after 29 hours.

in was introduced at 20 °C. The heating phase was subsequently modelled, and the outcomes were comparatively analysed after 29 hours.

in was introduced at 20 °C. The heating phase was subsequently modelled, and the outcomes were comparatively analysed after 29 hours.

in was introduced at 20 °C. The heating phase was subsequently modelled, and the outcomes were comparatively analysed after 29 hours.

in was introduced at 20 °C. The heating phase was subsequently modelled, and the outcomes were comparatively analysed after 29 hours.

in was introduced at 20 °C. The heating phase was subsequently modelled, and the outcomes were comparatively analysed after 29 hours.

in was introduced at 20 °C. The heating phase was subsequently modelled, and the outcomes were comparatively analysed after 29 hours.

in was introduced at 20 °C. The heating phase was subsequently modelled, and the outcomes were comparatively analysed after 29 hours.

in was introduced at 20 °C. The heating phase was subsequently modelled, and the outcomes were comparatively analysed after 29 hours.

in was introduced at 20 °C. The heating phase was subsequently modelled, and the outcomes were comparatively analysed after 29 hours.

in was introduced at 20 °C. The heating phase was subsequently modelled, and the outcomes were comparatively analysed after 29 hours.

in was introduced at 20 °C. The heating phase was subsequently modelled, and the outcomes were comparatively analysed after 29 hours.

in was introduced at 20 °C. The heating phase was subsequently modelled, and the outcomes were comparatively analysed after 29 hours.

in was introduced at 20 °C. The heating phase was subsequently modelled, and the outcomes were comparatively analysed after 29 hours.

in was introduced at 20 °C. The heating phase was subsequently modelled, and the outcomes were comparatively analysed after 29 hours.

in was introduced at 20 °C. The heating phase was subsequently modelled, and the outcomes were comparatively analysed after 29 hours.

in was introduced at 20 °C. The heating phase was subsequently modelled, and the outcomes were comparatively analysed after 29 hours.

in was introduced at 20 °C. The heating phase was subsequently modelled, and the outcomes were comparatively analysed after 29 hours.

in was introduced at 20 °C. The heating phase was subsequently modelled, and the outcomes were comparatively analysed after 29 hours.

Results

Heating Wire

Laboratory Experiment

Fig. 17 demonstrates the temperature distribution at the interface between the wood and casting resin. This is determined by a numerical simulation based on material properties for the cured

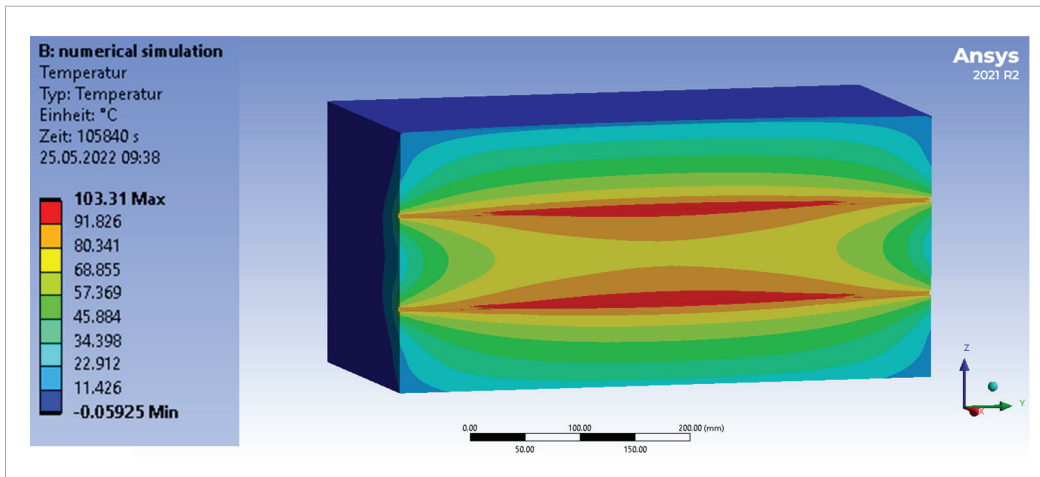


Fig. 17

Results numerical
 Analysis: Temperature
 Distribution after 29 h

state of the casting resin after 29 hours, at which stage a stable temperature distribution has been established. The visual representation uses a colour gradient to depict various temperatures, with red representing the highest temperatures and blue indicating the lowest. A clear temperature pattern is observable, with the heating wires showing the highest temperatures (reaching around 100 °C), while the outer surfaces record the lowest temperatures, consistent with the ambient temperature of 0 °C. Vertically along the testing object, the temperature reduces gradually from the heating wires outward and to a lesser extent between them, with a temperature difference of approximately 20 Kelvin. Furthermore, there is a detectable reduction in temperature from the inside to the exterior of the test sample.

Fig. 18 shows the vertical temperature profile of the test specimen obtained by analysing data gathered from its midpoint (aligned with its length). This figure also highlights a comparative explanation of the temperature readings obtained during the laboratory-based validation process. Upon initial inspection, similarities between the simulation and experimental trends are evident, yet a significant temperature discrepancy exists within certain areas. Specifically, there is an approximate 15 Kelvin difference in temperature at the heating wires and almost 40 Kelvin in the middle section. Even at the outer edges of the load-bearing lamellae (35 mm from the outer edge), there is a temperature difference of approximately 25 Kelvin.

However, Fig. 19 illustrates the comparison of the modified numerical simulation, in which the properties of the casting resin have been adjusted, with the experimental results. It is worth noting that there is a significantly enhanced level of correspondence between the simulation and the experiment. In both instances, the simulation aligns closely with the two outermost measurement points and one of the two points located at the heating wire also demonstrates excellent agreement. Nevertheless, there is a slight deviation of around 5 Kelvin at the other heating wire point, while the temperature measured between the heating wires is reported to be approximately 7 Kelvin lower in the experimental data when compared to the simulation. The differences

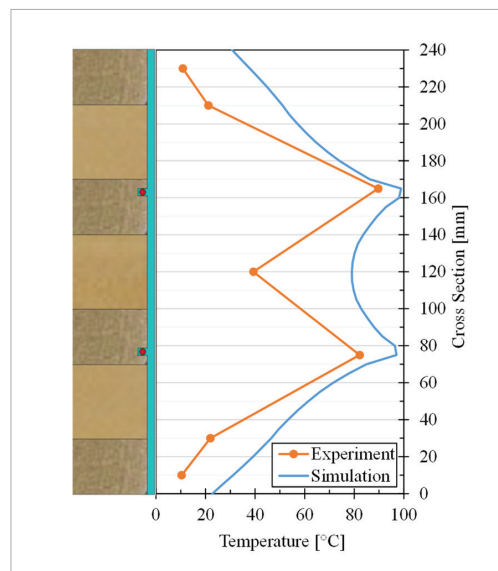


Fig. 18

Comparison Laboratory
 Experiment - Simulation:
 Temperature vs. Cross
 Section after 29 h

Fig. 19

Comparison Laboratory
Experiment -
adapted Simulation:
Temperature vs. Cross
Section after 29 h

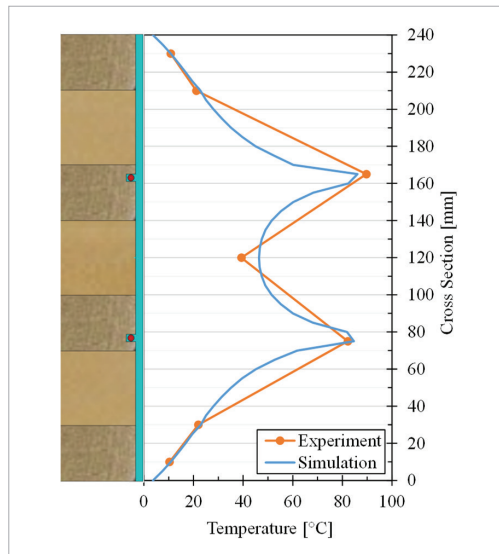


Fig. 20

Comparison Laboratory
Experiment - Simulation:
Temperature vs. Cross
Section after 29 h

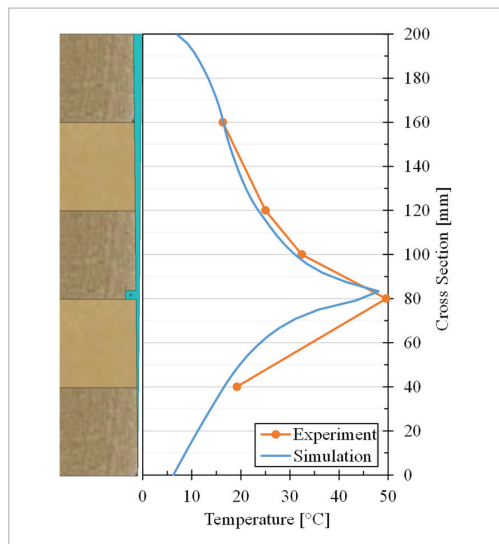
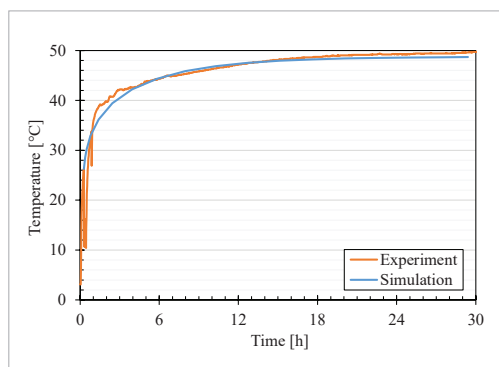


Fig. 21

Comparison Construction
Site Validation – adapted
Simulation: Temperature
vs. Time (measurement
point on the heating wire)



between the curves mainly arise from the simulation's capacity to provide a continuous profile, as opposed to the experiment, where data points were linearly linked.

On-site Validation

Fig. 20 shows the comparison of the cross-sectional temperature profiles from the adapted numerical simulation and on-site validation. This comparison is similar to previous ones and taken after the temperature has reached a stable state for 29 hours. The temperature reaches a peak of around 50 °C near the heating wire and gradually decreases towards the edges. Even at the outermost points of the external load-bearing lamellae, temperatures remain at around 20 °C. It's noteworthy that the measuring locations closely match the simulation, differing by only a few Kelvins. Additionally, Fig. 21 illustrates the timeline of temperature changes for the initial 29 hours after casting near the heating wire, thus providing another comparison between the simulation and on-site validation. The temperature gradually increases from roughly 0 °C during casting and eventually reaches approximately 50 °C after about 24 hours. This pattern shows similarities to a traditional instance of restricted development. The simulation and experiment once again confirm a strong correlation.

Hot Air Blower

Fig. 22 and Fig. 23 illustrate the results of the hot air blower tests for both variations. The temperature data was measured at all five points, ranging from 0.5 to 2.5 °C prior to the initiation of the hot air blowing process. The diagram shows, contrary to expectations, a distinct decrease in temperature during the three-minute blowing phase at four of the five measuring points. The temperature differences recorded among measuring points 1 - 3 are of about 1.0 K. During hot air dryer use, measuring point 5 drops by about 3.5 K, while only measuring point 4 shows a minor temperature increase of roughly 0.5 K. After deactivation of the hot air dryer, all measuring points return to their original temperatures within roughly 3 minutes, regardless of whether the tape is closed or cut.

temperature increase of roughly 0.5 K. After deactivation of the hot air dryer, all measuring points return to their original temperatures within roughly 3 minutes, regardless of whether the tape is closed or cut.

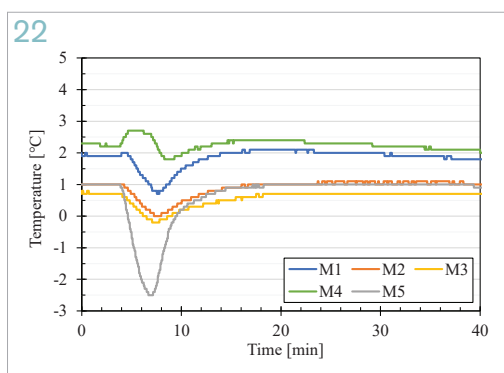


Fig. 22

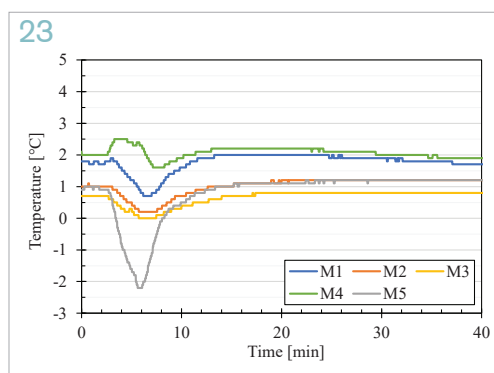
Temperature vs.
Time; closed Tape

Fig. 23

Temperature vs.
Time; cut Tape

Heating Wire

The findings, derived from simulations and experimental validations using milled heating wires, offer highly credible results. The evidence demonstrates a strong correlation between the adapted simulation outputs and validation results in the shown formats. It is crucial to acknowledge, however, that the material parameters, which were presumed constant throughout this study, indeed evolve over time under real-world conditions. Each of the characteristic values undergoes continuous transformations from the moment of component mixing until the casting resin achieves full cure and only stabilises thereafter. Moreover, there is a temperature dependency of these values present during both the curing phase and the fully cured state. However, the preceding analysis neglected both effects for the sake of simplicity. In summary, the simulation uses average material property values during the initial 29 hours after component mixing. This allows it to accurately predict temperature distribution at this time. The simulation achieves its purpose with good accuracy, and even the progression of temperature over time can be forecasted. However, ensuring the integrity and functionality of the heating wires throughout the intended heating period is essential. To monitor this, a method involves using temperature sensors distributed across the cross section, as demonstrated in the experiments which would introduce significant complexity.

Hot Air Blower

Contrary to expectations, the hot air dryer caused a temperature reduction at the measurement points, prompting several hypotheses. One plausible assumption is that the air blown in, with limited heat storage capacity ($\approx 1.005 \text{ kJ/kgK}$, Kuchling, 2010), cooled considerably during passage through the 30 cm-long filling hole, in close proximity to the cold wood, before reaching ambient temperature. It is possible that cold ambient air was drawn in and mixed with the warm air during the blowing process, leading to an intensified cooling effect and potentially explaining the lack of a temperature increase within the joint. However, this does not account for the decrease in temperature. Notably, the relative humidity in the climatic chamber set at around 0°C was approximately 60%. When utilising the hot air blower, the door to the chamber required opening, resulting in a slight temperature increase and significant rise in relative humidity. The augmented humidity in the blown air, in conjunction with the cooling effect as it flowed through the filling hole, conceivably caused the temperature sensors to record a lower reading due to the interaction of the amplified airflow velocity and humidity. Although the aforementioned effect is not anticipated in the construction field, it is justifiable to deduce that the implementation of a hot air blower does not significantly increase the temperature of the joint, making it an unfeasible remedy in practical scenarios.

Experiments utilising embedded heating wires show evidence establishing the efficacy of this technique in achieving the required curing temperature within the joint, even in low ambient temperatures. Additionally, tailored numerical simulations that assess temperature distribution over time across the cross section highly correlate with actual outcomes, demonstrating predictability.

Discussion

Conclusions and Outlook

Notably, this validity extends beyond laboratory-controlled conditions to genuine construction site scenarios. Therefore, it is feasible to predict the needed heating wire configurations according to environmental factors and enable an informed design of the heating wire system. On the other hand, the second option being examined, which involves using a hot air blower, does not appear to offer a promising compensatory measure. This is because there is no significant effect resulting from this approach. The heating wire method is a feasible approach, despite the substantial extra workload associated with milling, installation, heating wire adjustment, and quality assurance. Since these endeavours are comprehensive, researchers are continuously exploring alternative methods for achieving bonding at lower ambient temperatures with less complexity.

Acknowledgment

This research project could be established and realised in collaboration between the main industrial partner Timber Structures 3.0 AG together with Schilliger Holz AG, Henkel & Cie. AG supported by the Bern University of Applied Sciences, and ETH Zürich and significant funding by Innosuisse (Application Number: 50393.1 IP-ENG). At this point, a heartfelt thank you from the authors for the constructive and trusting cooperation, support and funding.

References

- Deutsches Institut für Bautechnik. (2020). 2K-PUR Klebstoff LOCTITE CR 821 PURBOND zum Einkleben von Stahlstäben in tragende Holzbauteile. Allgemeine bauaufsichtliche Zulassung Z-9.1-896.
- Klima und Wetter in Europa. (2023). Wetter Atlas. <https://www.wetter-atlas.de/klima/europa.php>
- Kuchling, H. (2010). Taschenbuch der Physik. Fachbuchverlag Leipzig.
- Lins, D., Franke, S. (2023). Influence of low curing temperatures on the strength development of end-grain bonded timber. Word Conference on Timber Engineering 2023, Oslo, Norway. <https://doi.org/10.52202/069179-0177>
- Niemz, P. (2005). Physik des Holzes. ETH Zürich.
- References. (2023). TS3. <https://www.ts3.biz/en/referenzprojekte/>
- Technology. (2023). TS3. <https://www.ts3.biz/en/technologien/>

About the Authors

DIO LINS

PhD student

Bern University of Applied Sciences
Institute for Timber Construction

Main research area

End-grain bonding of timber components,
timber connections

Address

Solothurnstrasse 102
CH-2504 Biel
E-mail: dio.lins@bfh.ch

STEFFEN FRANKE

Professor for Timber Engineering and Static Design

Bern University of Applied Sciences
Institute for Timber Construction

Main research area

Timber connections, product developments,
monitoring

Address

Solothurnstrasse 102
CH-2504 Biel
E-mail: steffen.franke@bfh.ch

